Large Eddy Simulation in a Split Form Discontinuous Galerkin Method for the Compressible Navier-Stokes

Anthony Edmonds
Masters Defense
Department of Mechanical Engineering

University of Wyoming

Motivation

- Turbulence is prevalent in every day life
  - Most common engineering flow
- Characterized by:
  - Mechanical mixing
  - Vorticies
  - Chaotic fluctuations
  - Cascade of Energy from large to small scales
- These characteristics are a challenge to simulate

Motivation

- An accurate simulation must capture all temporal and spatial scales
  - Computationally expensive
- Large Eddy Simulation
  - Reduced computational cost
  - Without sacrificing accuracy
  - Two LES models were analyzed
    - Constant Smagorinsky
    - Dynamic Smagorinsky

Motivation

- High order finite element methods (FEM) have grown in popularity
  - FEM can leverage new architectural advances
  - Historically neglected due to high computational costs
- The Discontinuous Galerkin Method is a finite element method with discontinuous values at each element interface
  - Relies on the weak form of the governing equations

Motivation

- An alternative DG formulation exists that relies on the strong form
  - The split-form is derived from the strong form DG
  - This split-form is kinetic energy preserving
- The behavior of the LES models when used with the split-form DG formulation were analyzed and compared to the standard DG formulation

Direct Numerical Simulation (DNS)

- All time and space scales are simulated
- Very fine mesh resolution required
- Very small time steps required
- Very Expensive
  - Everything is directly simulatied
  - Increasing Reynolds Number increases the cost

Reynolds Averaged Navier-Stokes (RANS)

- Average flow field is calculated
- Models the fluctuations
- Much cheaper due to the reduced resolution needed
- Struggles with unsteady flow problems
- Reduction of accuracy due to model limitations
- Models need to be selected correctly for a given problem

COLLEGE OF ENGINEERING & APPLIED SCIENCE
UNIVERSITY OF WYOMING

Large Eddy Simulation (LES)

- Directly simulate large scale structures
- Filter smallest scales (sub-grid scales)
- Introduce model for the SGS
- Cheaper than DNS, lower accuracy
- More expensive than RANS, more accuracy

Compressible Navier-Stokes

$$\frac{\partial \boldsymbol{Q}(x,t)}{\partial t} + \vec{\nabla} \cdot \boldsymbol{F}\big(\boldsymbol{Q}(x,t)\big) = 0$$

$$\boldsymbol{Q} = \begin{bmatrix} \rho \\ \rho u \\ \rho v \\ \rho w \\ \rho E \end{bmatrix}, \boldsymbol{F} = \begin{bmatrix} \rho u & \rho v & \rho w \\ \rho uu + P - \tau_{11} & \rho vu \ - \tau_{12} & \rho wu \ - \tau_{13} \\ \rho uv \ - \tau_{21} & \rho vv + P - \tau_{22} & \rho wv \ - \tau_{23} \\ \rho uw \ - \tau_{31} & \rho vw \ - \tau_{32} & \rho ww + P - \tau_{33} \\ \rho uH + q_1 - \tau_{1j} u_j & \rho vH + q_2 - \tau_{2j} u_j & \rho wH + q_3 - \tau_{3j} u_j \end{bmatrix}$$

$$q_i = -\frac{C_p \mu}{Pr} \frac{\partial T}{\partial x_i},$$

Weak Form

- Obtained by multiplying by a test function
$$\phi_s, s = 1, \ldots, M$$
- And integrating over the element volume

$$\int_{\Omega_k} \left(\frac{\partial \boldsymbol{Q}}{\partial t} + \vec{\nabla} \cdot \boldsymbol{F} \right) \phi(x)\, dx$$

Weak Form

- Separating and applying the divergence theorem

$$R^{weak} = \int_{\Omega_k} \frac{\partial \boldsymbol{Q}}{\partial t} \phi(x) dx$$

$$- \int_{\Omega_k} (\boldsymbol{F} \cdot \vec{\nabla}) \phi(x) dx$$

$$+ \int_{\boldsymbol{\Gamma}_\mathbf{k}} (\boldsymbol{F}^* \cdot \vec{n}) \phi\left(x|_{\Gamma_k}\right) d\Gamma_k = 0$$

Strong Form

- The divergence theorem is applied a second time to the volume term
- The derivative of the volume fluxes must now be calculated
- An additional term now must be evaluated at the boundary

Strong Form

$$R^{strong} = \int_{\Omega_k} \frac{\partial \boldsymbol{Q}}{\partial t} \phi(x) dx$$

$$- \int_{\Omega_k} (\vec{\nabla} \boldsymbol{F} \cdot \phi(x)) dx$$

$$+ \int_{\boldsymbol{\Gamma_k}} ((\boldsymbol{F}^* - \boldsymbol{F}) \cdot \vec{n}) \phi\left(x|_{\Gamma_k}\right) d\Gamma_k = 0$$

Split-Form

- The summation-by-parts property is applied to the surface fluxes on of the strong form discretization
- Requires a coordinate transform of the generalized governing equations:

$$J\frac{\partial \widetilde{\mathbf{Q}}}{\partial t} + \widetilde{\vec{\mathcal{L}}}_X(\mathbf{Q}) + \widetilde{\vec{\mathcal{L}}}_Y(\mathbf{Q}) + \widetilde{\vec{\mathcal{L}}}_Z(\mathbf{Q}) = 0$$

Split-Form

- The split-form discretization is derived from the DG spectral element formulation (DGSEM) and is constructed in a similar manner to the standard DG formulation

$$(\tilde{\vec{\mathcal{L}}}_X)_{i,j,k} \approx \frac{1}{\omega_i}(\delta_{iN}[\tilde{\mathcal{F}}^* - \tilde{\mathcal{F}}]_{Njk} - \delta i1[\tilde{\mathcal{F}}^* - \tilde{\mathcal{F}}]_{1jk} + \sum_{m=1}^{N} \mathbf{D}_{im}(\tilde{\mathcal{F}})_{mjk}$$

Pirozzoli Numerical Flux Scheme

- A split-form discretization only flux scheme
  - Primarily used with no artificial dissipation in this work

$$\tilde{\vec{\mathcal{L}}}_X^{\mathrm{PZ}}(Q) = \begin{bmatrix} \frac{1}{2}((\rho u)_x \rho(u)_x + u(\rho)_x) \\ \frac{1}{4}((\rho u^2)_x + \rho(u^2)_x + 2u(\rho u)_x + u^2(\rho)_x + 2\rho u(u)_x) + p_x \\ \frac{1}{4}((\rho uv)_x + \rho(uv)_x + u(\rho v)_x + v(\rho u)_x + uv(\rho)_x + \rho v(u)_x + \rho u(v)_x) \\ \frac{1}{4}((\rho uw)_x + \rho(uw)_x + u(\rho w)_x + w(\rho u)_x + uw(\rho)_x + \rho w(u)_x + \rho u(w)_x) \\ \frac{1}{4}((\rho uh)_x + \rho(uh)_x + h(\rho u)_x + u(\rho h)_x + uh(\rho)_x + \rho u(h)_x + \rho u(u)_x) \end{bmatrix}$$

Solution Filtering

- A method for stabilizing DG methods
- Solution is filtered at each time step
  - Also any time stepping stages like in the Runge-Kutta Method
- Solution filter is also used in the Dynamic Smagorinsky Method
  - Modal Cutoff
  - Laplacian Filter

Modal Cutoff Filter

- An Nth order hierarchical basis function contains all lower solutions
- Specific orders can be filtered by zeroing corresponding modes
- Emulates a sharp cut off filter
- Problem: CartDG uses a nodal basis for solution

Hierarchical Modal basis

- Legendre Polynomial used to calculate
- P6 Basis shown
- All lower order basis functions are represented in the basis

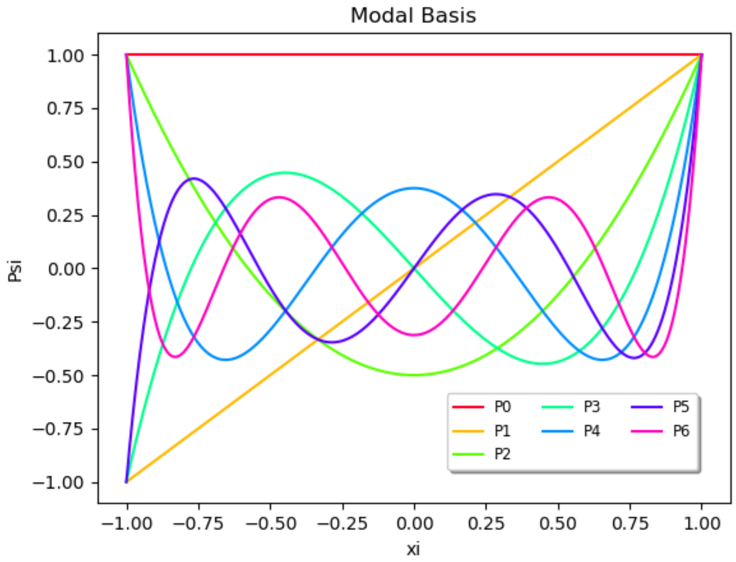

Nodal Basis

- Gives rise to Kronecker Delta Property used to speed up CartDG
- Each order has a unique set of basis functions
- P6 Basis shown

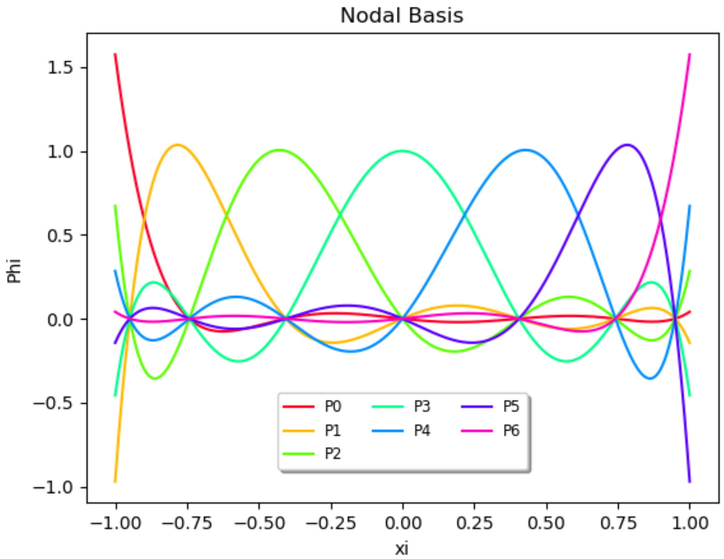

Modal Cutoff Filter

- Can be transformed by use of mass matricies
- Modal Mass Matrix

$$M_{ij} = \int_{-1}^{1} \psi_i(\xi)\psi_j(\xi)d\xi$$

- Mix Mass Matrix

$$C_{ij} = \int_{-1}^{1} \psi_i(\xi)\phi_j(\xi)d\xi$$

- This can be used to calculate

$$C\vec{u} = M\vec{b}$$
$$\vec{b} = M^{-1}C\vec{u}$$

- The filter matrix F can be applied

$$\bar{\vec{b}} = F\vec{b}$$

Modal Cutoff Filter

- This can be used to get the filtered solution

$$\overline{\vec{u}} = C^{-1}M\overline{\vec{b}}$$

$$\overline{\vec{u}} = C^{-1}MFM^{-1}C\vec{u}$$

- Terms can be combined into an overall filter $\hat{F}$

$$\overline{\vec{u}} = \hat{F}\vec{u}$$

- Filter $\hat{F}$ only needs to be calculated once

1-D Test Problem

- P6 Nodal approximation in Red
- N = 6 mesh elements (blue)
- Quadrature points shown in violet
- Black is true solution $y = \cos(2x) + 0.3\sin(8x) + \sin(x^2) + 0.4\sin\left(\frac{36}{\pi}x\right)$

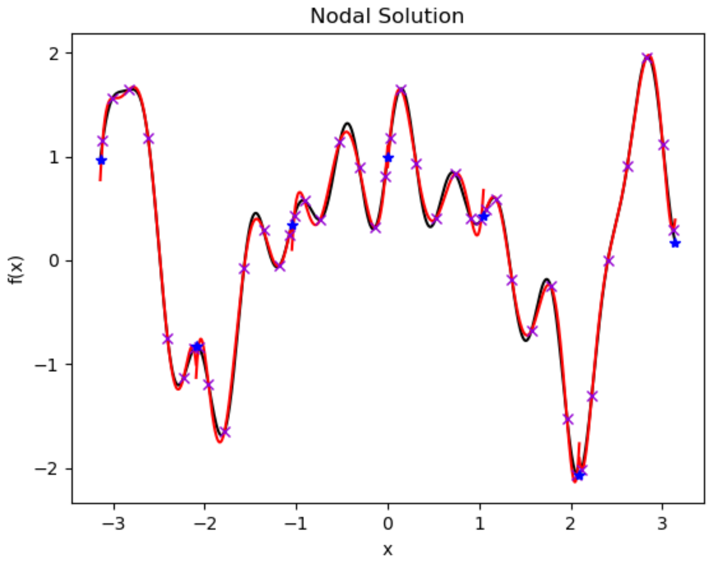

1-D Test Problem: Modal Cutoff Filter

- P4 filtered solution in green
- Steep peaks are smoothed out in several areas
- Some larger discontinuities near element boundary
- High order content is removed
- Solution is slightly less accurate

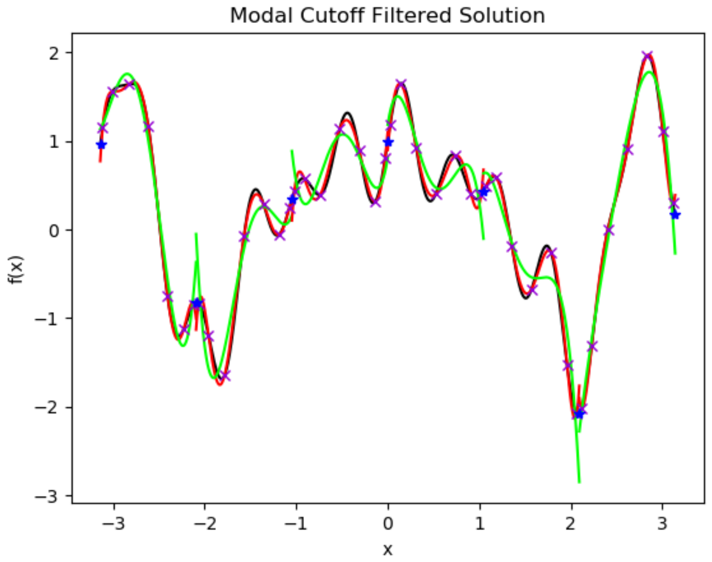

1-D Test Problem: Modal Cutoff Filter

- P1 filtered solution in green
- All high order frequencies are smoothed out
- Solution accuracy is poor
- Implies that too low of filter order worsens accuracy and potentially stability

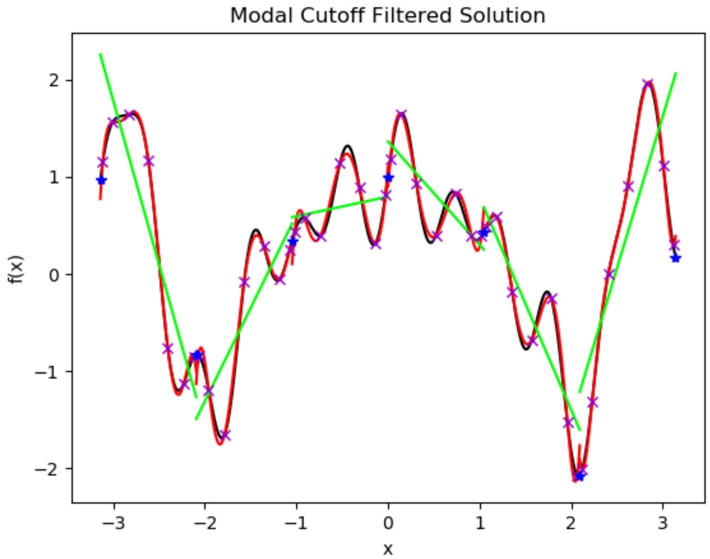

3-D Test Problem

- P6 Nodal approximation for x-momentum ρu
- Taylor Green Vortex
  - At $\tau \approx 10$
- N = 10 mesh elements in each direction
- Red is positive values of ρu, green is zero, and blue is negative values

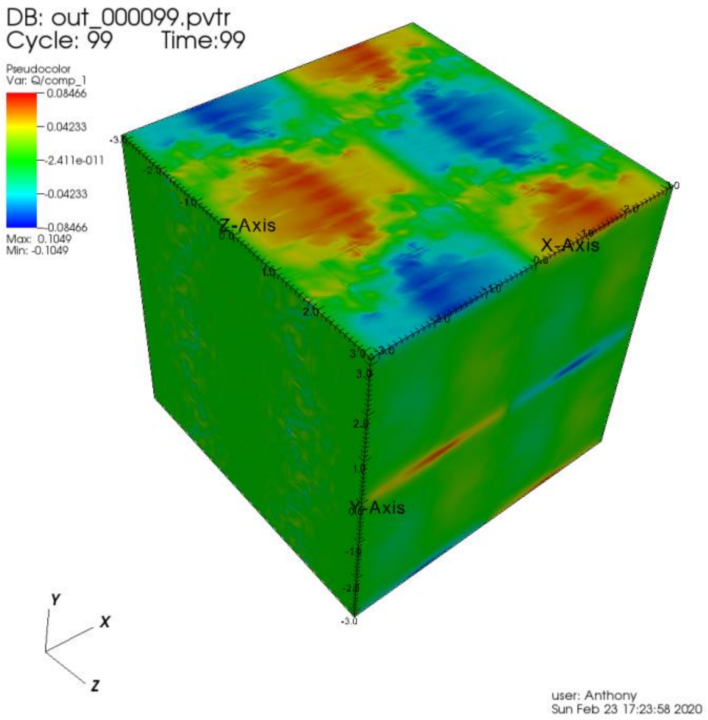

3-D Test Problem: Modal Cutoff Filter

- P4 filtered solution
- Sharp flow features smoothed out on XZ-face near Z = 0
- Majors structures on XZ-face have become more defined

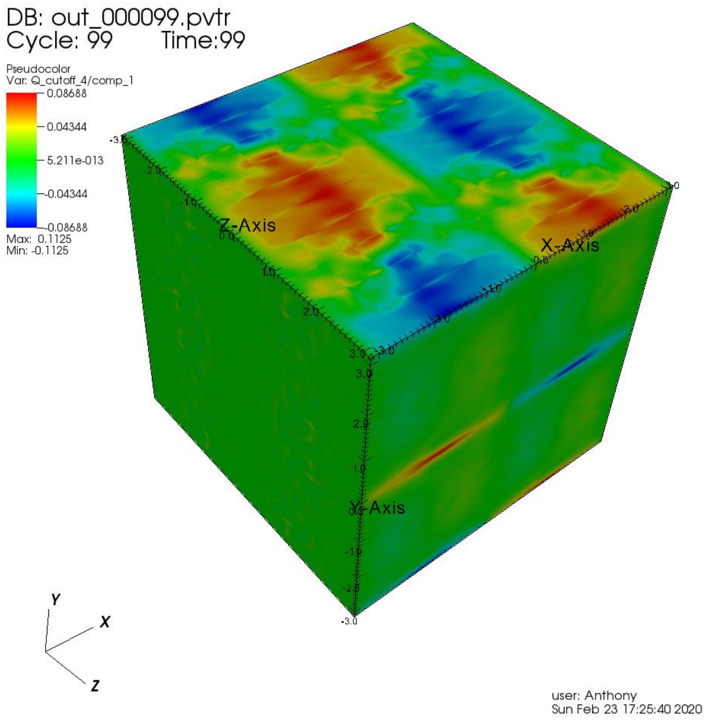

3-D Test Problem: Modal Cutoff Filter

- P1 filtered solution
- Structures are coarse
- Other structures smoothed out entirely
- Discontinuities from finite representation are apparent
- Suggest that too low of a filter order leads to a significant degradation in accuracy

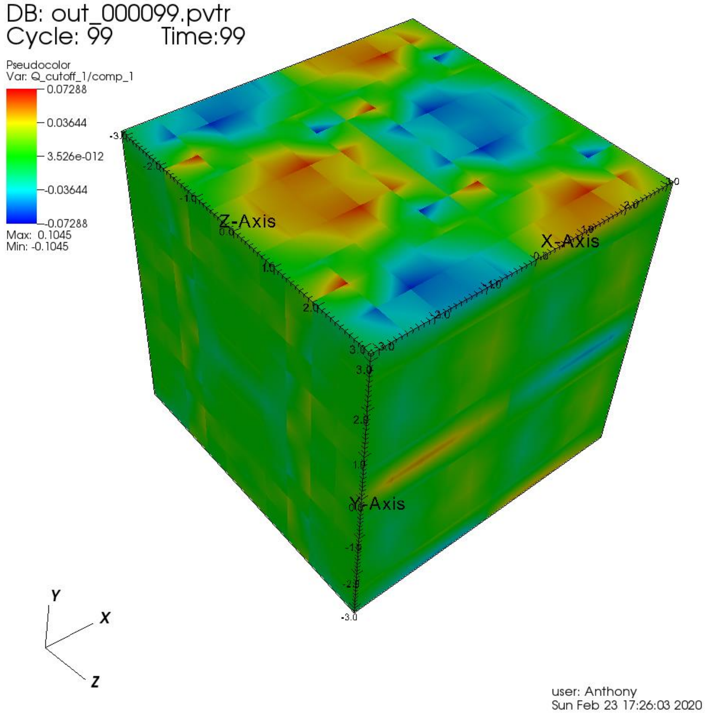

Laplace Filter

- Regularizations of the convective term in the Navier-Stokes equations
  - This nonlinear term leads to the small scale structures for the turbulent cascade
- The regularization of this term can lead to the convection term becoming a source or a sink
  - This can be corrected by projecting onto a divergence free space
- This lead to this work investigating the Laplace Filter in the dynamic Smagorinsky model

Laplace Filter

- Calculated explicitly:

$$\bar{u} = u + \nabla \cdot (\gamma \nabla u)$$

- Where the filtered solution $\bar{u}$ is filtered based on the divergence of the flow
- γ is a filter width term
  - Box filter was selected on a per element basis

$$\gamma = \frac{\left(\frac{1}{p+1} \times (\Omega_k)^{\frac{1}{3}}\right)^2}{24}$$

- With the element volume Ω_k normalized by the solution order p

1-D Test Problem

- P6 Nodal approximation in Red
- N = 6 mesh elements (blue)
- Quadrature points shown in violet
- Black is true solution $y = \cos(2x) + 0.3\sin(8x) + \sin(x^2) + 0.4\sin\left(\frac{36}{\pi}x\right)$

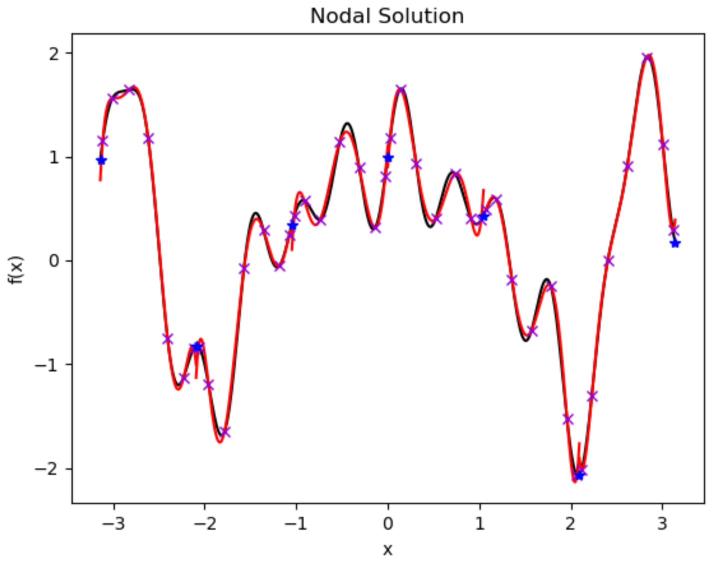

1-D Test Problem: Laplace Filter

- Laplacian filtered solution in green
- Minimal changes in filtered solution
  - Derivative of a sinusoid is a sinusoid
- Slight changes near the edges of each element

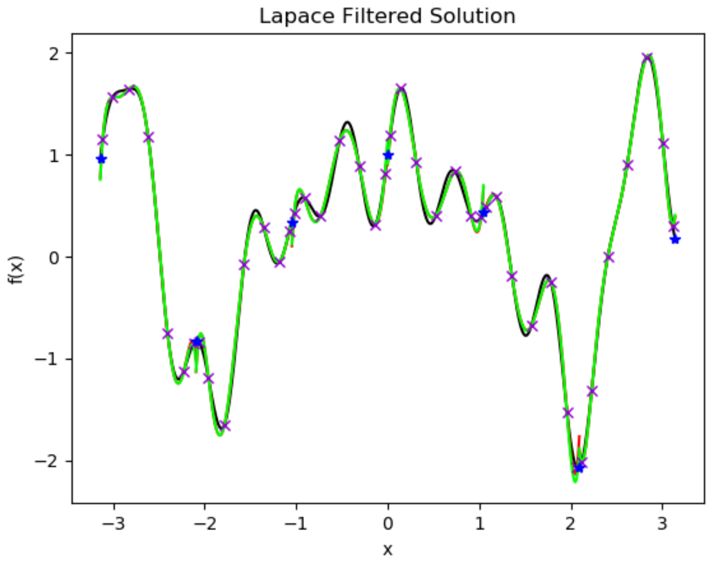

3-D Test Problem

- P6 Nodal approximation for x-momentum ρu
- Taylor Green Vortex
  - At $\tau \approx 10$
- N = 10 mesh elements in each direction
- Red is positive values of ρu, green is zero, and blue is negative values

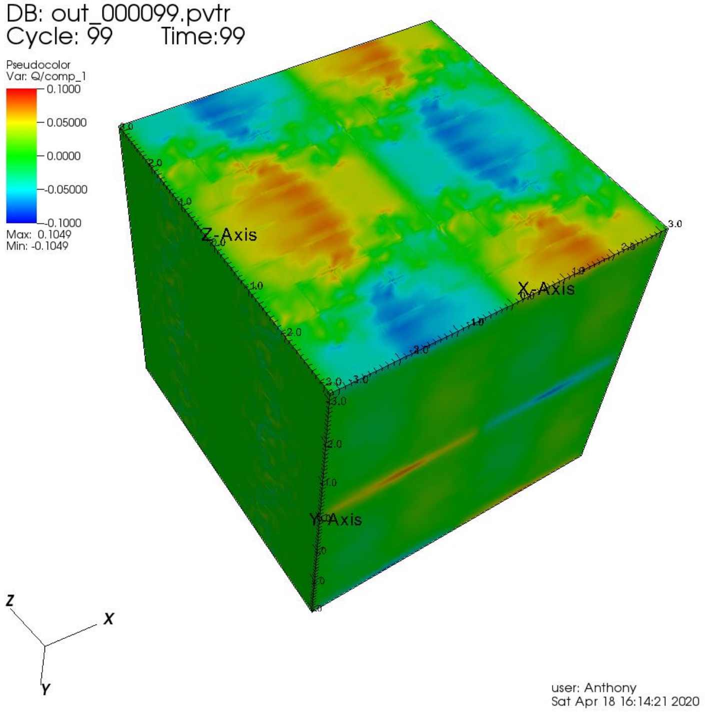

3-D Test Problem: Laplace Filter

- Laplace filtered solution
- Formerly smooth areas now have structures
  - These arise from small changes in the sign of the solution
- Areas with more gradual changes are smoothed out
- This makes it ideal for the filter used in LES
  - These areas are more likely to be under resolved

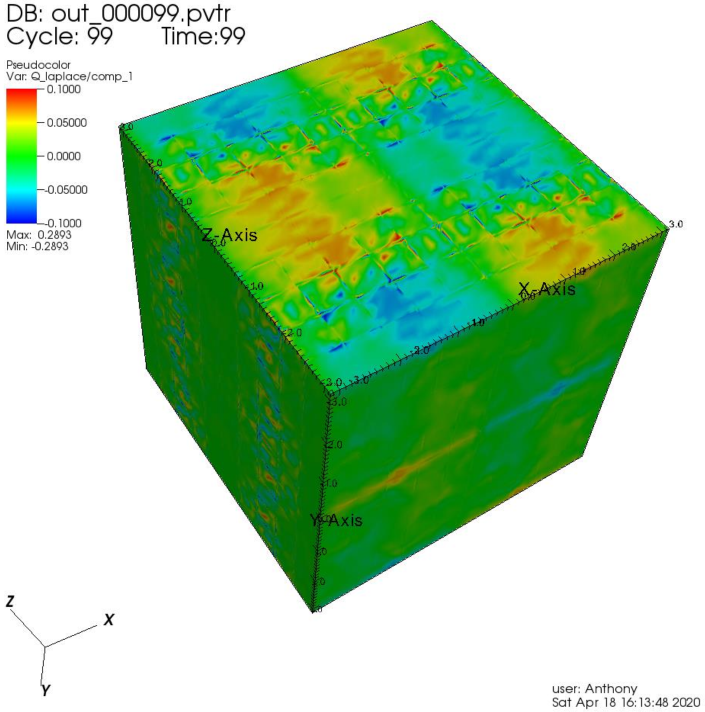

LES Equations

- To obtain these equations a low-pass filter is applied to the Navier-Stokes equations
  - Applied to the incompressible Conservation of Mass:

$$\overline{\frac{\partial u_i}{\partial t} + \frac{\partial u_i u_j}{\partial x_j}} = \overline{-\frac{1}{\rho}\frac{\partial p}{\partial x_i} + 2\nu\frac{\partial S_{ij}^d}{\partial x_j}}$$

LES Equations

- The filter is linear:

$$\overline{\frac{\partial u_i}{\partial t}} + \overline{\frac{\partial u_i u_j}{\partial x_j}} = \overline{-\frac{1}{\rho}\frac{\partial p}{\partial x_i}} + \overline{2\nu \frac{\partial S^d_{ij}}{\partial x_j}}$$

- Commutative with respect to differentiation:

$$\frac{\partial \overline{u_i}}{\partial t} + \frac{\partial \overline{u_i u_j}}{\partial x_j} = -\frac{1}{\rho}\frac{\partial \overline{p}}{\partial x_i} + 2\nu \frac{\partial \overline{S^d_{ij}}}{\partial x_j}$$

LES Equations

- This filter operation introduces $\overline{u_i u_j}$ as an unknown
- This is approximated by decomposing the term into:

$$\tau_{ij} = \overline{u_i u_j} - \bar{u}_i \bar{u}_j$$

- τ_{ij} is the sub-grid scale (SGS) stress tensor
- The deviatoric SGS stress tensor can be calculated with:

$$\tau_{ij}^d = -2\,\nu_{SGS} \overline{S_{ij}^d}$$

- Which introduces ν_{SGS} as the eddy viscosity or sub-grid scale kinematic viscosity
- An LES model is introduced to solve for ν_{SGS}
- The same procedure can be followed for compressible LES but requires the use of Favre filtering

Favre Filtering

- Key for LES in compressible flows
- Change of variables based on filtered density
- This can be written as:

$$\overline{\rho\Phi} = \bar{\rho}\widetilde{\Phi}$$

- Or more practically:

$$\widetilde{\Phi} = \frac{\overline{\rho\Phi}}{\bar{\rho}}$$

Constant Smagorinsky Model

- Directly models μ_{SGS} based on instantaneous flow state:

$$\mu_{SGS} = \bar{\rho}(C_s\Delta)^2|\tilde{S}|$$

- $|\tilde{S}|$ is the magnitude of the Favre averaged strain rate tensor:

$$|\tilde{S}| = \sqrt{2\widetilde{S_{ij}}\widetilde{S_{ij}}}$$

Constant Smagorinsky Model

- C_s is the Smagorinsky coefficient
  - Often chosen to be 0.17
- Δ represents the element size

$$\Delta = C_P\left(\Delta_x \Delta_y \Delta_z\right)^{1/3}$$

- C_P factors in finite element solution order P:

$$C_P = \frac{1}{P+1}$$

Dynamic Smagorinsky Model

- Modification of the constant Smagorinsky model
  - Constant model poorly handles laminar and transitional flows
- The Smagorinsky coefficient is now calculated as a function of the instantaneous flow state

$$C_s = C_s(x, y, z, t)$$

- An explicit filter operation is applied locally
  - Occurs independently of solution or grid filtering
  - This filter is referred to as the test filter

Dynamic Smagorinsky Model

- This work examined the performance both filters
  - Sharp Modal Cutoff
  - Laplace
- Test filtered quantity is represented by a hat

$$\hat{\bar{\rho}}$$

- Calculation is based on the Leonard Stress tensor:

$$L_{ij} = \widehat{\bar{\rho}\tilde{u}_i\tilde{u}_j} - \frac{\widehat{\bar{\rho}\tilde{u}_i}\,\widehat{\bar{\rho}\tilde{u}_j}}{\hat{\bar{\rho}}}$$

- And the M_{ij} tensor:

$$M_{ij} = \left(\widehat{\bar{\rho}|\tilde{S}|\tilde{S}^{d}_{ij}}\right) - \alpha\hat{\bar{\rho}}\left|\hat{\tilde{S}}\right|\widehat{\tilde{S}^{d}_{ij}}$$

Dynamic Smagorinsky Model

- α is the ratio of the grid filter size and the test filter size:

$$\alpha = \left(\frac{\widehat{\tilde{\Delta}}}{\bar{\tilde{\Delta}}}\right)^2$$

- For the finite element formulation order is factored in:

$$\alpha = \left(\frac{p_{grid} + 1}{p_{test} + 1}\right)^2$$

- Manipulation of the terms results in:

$$(C_s\Delta)^2 = \frac{1}{2}\frac{L_{ij}^{d} M_{ij}}{M_{lk} M_{lk}}$$

- Which is then substituted into:

$$\mu_{SGS} = \bar{\rho}(C_s\Delta)^2\left|\tilde{S}\right|$$

Dynamic Smagorinsky Model

- Both tensors are constructed out of terms:
  - Filtered then assembled
  - Assembled then filtered
- High energy content is associated with high order components of flow
- Leonard Stress tensor becomes zero in smooth flow
  - Results in ν_{SGS} having zero contribution in this flow regime
  - This contrasts with the Constant model that only has zero contribution with zero strain rate

Dynamic Smagorinsky Model

- Calculated at each integration point, then averaged over the volume:

$$\langle (C_s\Delta)^2 \rangle_e = \frac{\int_{V_e} (C_s\Delta)^2 dV}{V_e}$$

- Then applied on a per element basis
- Clipping was introduced to prevent μ_{SGS} from becoming negative
  - If $\mu + \mu_{SGS} \leq \mathbf{0}$ instabilities will form

Implicit Large Eddy Simulation

- ILES relies strictly on the native viscosity from the Navier-Stokes equations and numerical dissipation arising from the solver
- No small scale physics or structures are captured
- Referred to as *Baseline* or *No Model* in this work

Taylor Green Vortex

- Is an unsteady flow that is initially laminar and under goes transition to fully turbulent flow
- Ideal test for SGS models
  - Transition is difficult to handle
- Inherently an incompressible problem
  - Mach Number of 0.1 was selected

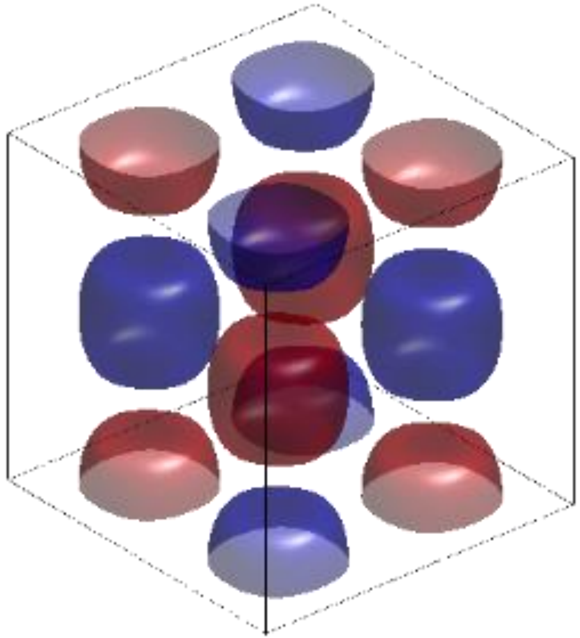

Contour of Z-vorticitiy at the initial condition [1].

Taylor Green Vortex

- This is a perodic problem
  - All boundary conditions were perodic
- Domain of $[-\pi L, \pi L] x [-\pi L, \pi L] x [-\pi L, \pi L]$
  - With the characteristic length L = 1.0
- The Characteristic velocity $U_0 = 0.1$
- The initial density $\rho = 1.0$
- Air was chosen as the working fluid
  - $\gamma = 1.4$
  - Pr = 0.71

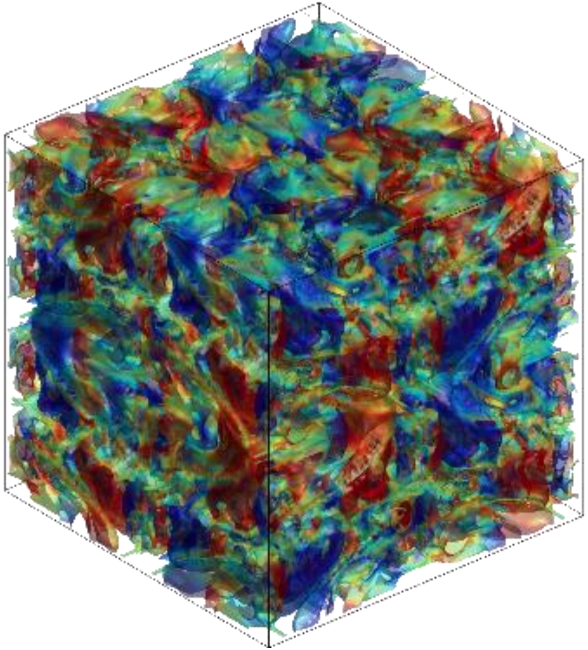

Contour of Z-vorticitiy at $\tau = 20.0$ condition [1].

Taylor Green Vortex

- Initial Flow field:

$$u = U_0 sin(\frac{x}{L}) cos(\frac{y}{L}) cos(\frac{z}{L})$$

$$v = U_0 cos(\frac{x}{L}) sin(\frac{y}{L}) cos(\frac{z}{L})$$

$$w = 0$$

$$P = P_0 = \frac{\rho_0 U_0^2}{16} \left(cos\left(\frac{2x}{L}\right) + cos\left(\frac{2y}{L}\right)\right)\left(cos\left(\frac{2z}{L}\right)\right)$$

Taylor Green Vortex

- Initial temperature was considered to be uniform
  - Thus density was calculated by:

$$\rho = RT_0$$

- The time was normalized with a characteristic convective time:
  - $t_c = L/U_0$
  - $\tau = \frac{t}{t_c}$

Taylor Green Vortex

- Key quantities were analyzed to determine the behavior of the TGV simulation runs
- Volume averaged kinetic energy:

$$KE = \frac{1}{\rho\Omega}\int_{\Omega} \rho \frac{u_i u_j}{2} d\Omega$$

- Kinetic energy dissipation rate:

$$\epsilon = -\frac{dK}{dt}$$

Taylor Green Vortex

- Kinetic energy rate is based on the sum of three terms:
  - The e_1 term represents the dissipation arising from viscosity:

$$e_1 = \frac{2}{\rho_0 \Omega} \int_\Omega \mu S_{ij}^d S_{ij}^d d\Omega$$

  - The e_2 term represents dissipation arising from velocity dilatation:

$$e_2 = \frac{2\mu}{3\rho_0 \Omega} \int_\Omega (\nabla \cdot u)^2 d\Omega$$

  - The e_3 term represents dissipation arising from pressure dilatation:

$$e_3 = -\frac{1}{\rho_0 \Omega} \int_\Omega P(\nabla \cdot u) d\Omega$$

- Due to the incompressible nature of the problem e_2 and e_3 should be negligible

Taylor Green Vortex

- Volume averaged turbulent viscosity was also analyzed:

$$\overline{\mu_{SGS}} = \frac{1}{\Omega}\int_{\Omega} \mu_{SGS} d\Omega$$

- The number of degrees of freedom were calculated as:

$$DOF = [(P+1)n_{1D}]^3$$

  - This is based on the solution order P and the number of elements which were constant for each direction

Taylor Green Vortex

- Simulations were run in CartDG
- Both the split-form and standard DG discretizations were run
- The explicit fourth-order four stage Runge-Kutaa (RK4) scheme was used for time advancement
  - The 3/8th Method was used for the RK coefficients
- CFL = 1.0 was selected

Inviscid Taylor Green Vortex

- TGV was run without viscosity
- Fully periodic
- No means of dissipating energy
  - TKE should be strictly conserved
- Challenging:
  - Will always be under-resolved for long simulations

Results: Inviscid TGV DG

- Total Kinetic Energy
- Run with the standard DG formulation
- Lax-Friedrichs numerical flux scheme
- All cases P2, P3, and P6 filtered to P3 are too dissipative
- Only the lowest order P2 case, shown in purple, was stable and ran to completion

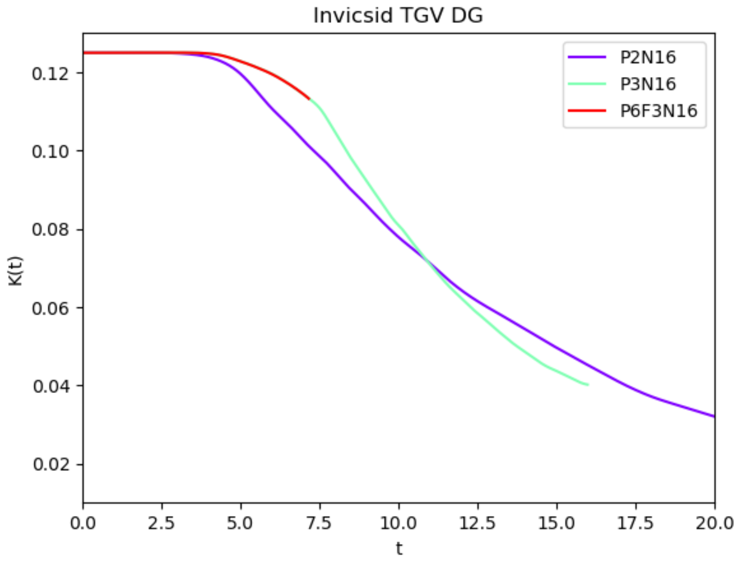

Results: Inviscid TGV DG

- P3, shown in green, reaches approximately $\tau \approx 16.0$ before crashing
- Adding in filtering from P6 to P3, shown in red, destabilized the solution further
  - Due to worsening polynomial aliasing errors
  - The quadrature points are as if the solution was P6

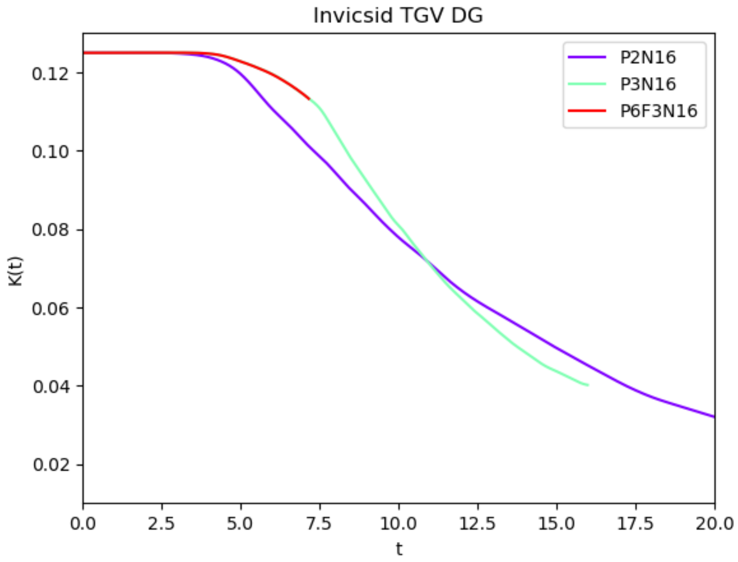

Results: Inviscid TGV Split-form

- Total Kinetic Energy
- Run with the split-form
- No numerical flux dissipation was introduced
- P2, shown in purple, runs to completion
  - Negligible changes in KE
- P3, shown in cyan, runs to completion
  - KE begins to decrease at $\tau \approx 13.0$
  - Then begins to rise after $\tau \approx 18.0$

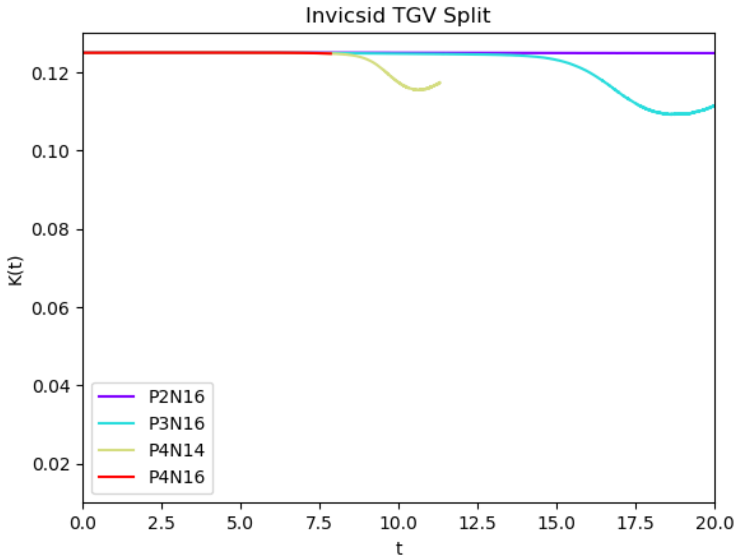

Results: Inviscid TGV Split-form

- Both P4 cases crash
- The case with 14 elements per direction shown in yellow
    - Preserves KE until $\tau \approx 7.5$
    - At this point it decreases
    - It begins to increase at $\tau \approx 10.0$ before crashing
- The case with 16 elements per direction
    - Preserves KE for its entire life before crashing

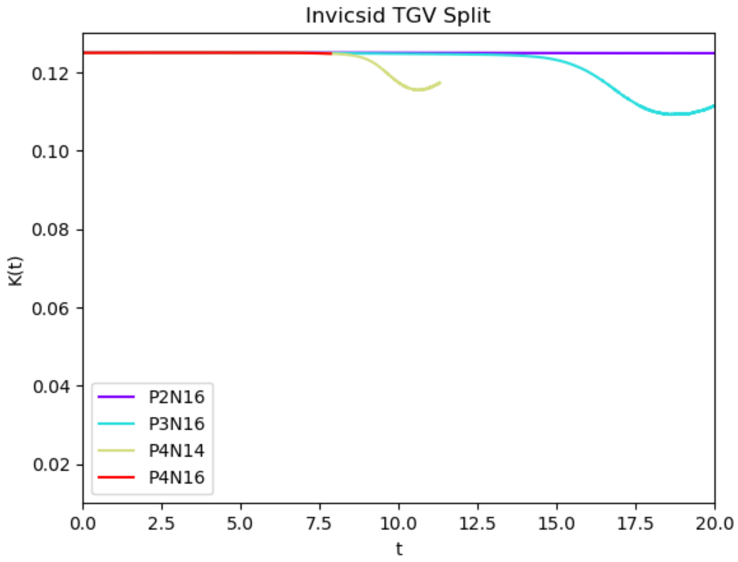

Taylor Green Vortex

- Run with viscosity
- Reynolds Number was varied to examine the effects
  - RE=1,600
  - RE=20,000
- Run with and without LES models
  - Baseline will refer to ILES

Results: TGV DG

- Run with viscosity
- Reynolds Number was varied to examine the effects
  - RE=1,600
  - RE=20,000
- Run with and without LES models
  - Baseline will refer to ILES

Results: TGV DG vs Split-Form

- TKE with Re-20000 P6
  - DNS is in Purple
  - Standard DG formulation in green
  - Split-form in red
- The standard DG formulation is unstable
  - In the regime before the instability is more accurate then the split-form

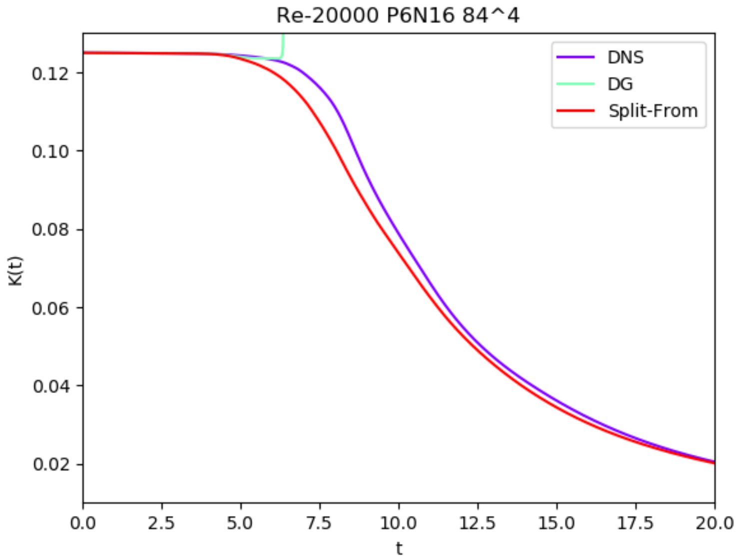

Results: TGV DG vs Split-Form

- The split-form under predicts compared to the DNS
  - The transition is predicted earlier

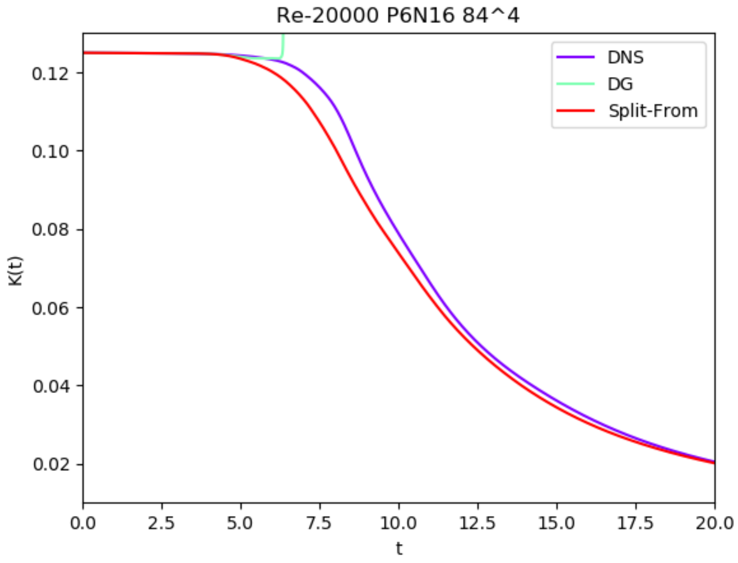

Results: TGV Split-form LES

- Total Kinetic Energy at Re=1,600
  - DNS results are in purple
  - Baseline simulation with no LES model is shown in Blue
  - The simulation with Constant Smagorinsky model model is green
  - The simulation with Dynamic Smagorinsky model with the modal cutoff filter set to P4 is in orange
  - The simulation with Dynamic Smagorinsky model with the Laplacian filter is in red

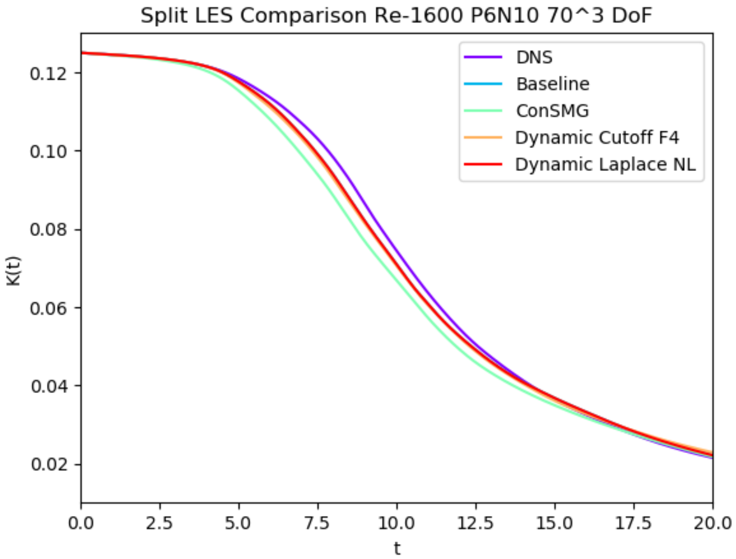

Results: TGV Split-form

- All simulations
  - under predict KE compared to the DNS
  - predict transition earlier than the DNS
- The Constant Smagorinsky Model is the most under predictive
  - It predicts transition the earliest
- The Dynamic Smagorinsky Model with the modal cutoff filter is slightly more dissipative than the baseline, the split-form with no model
- The Dynamic Smagorinsky Model with the Laplace Filter is nearly identical to the baseline as the model has very little contribution

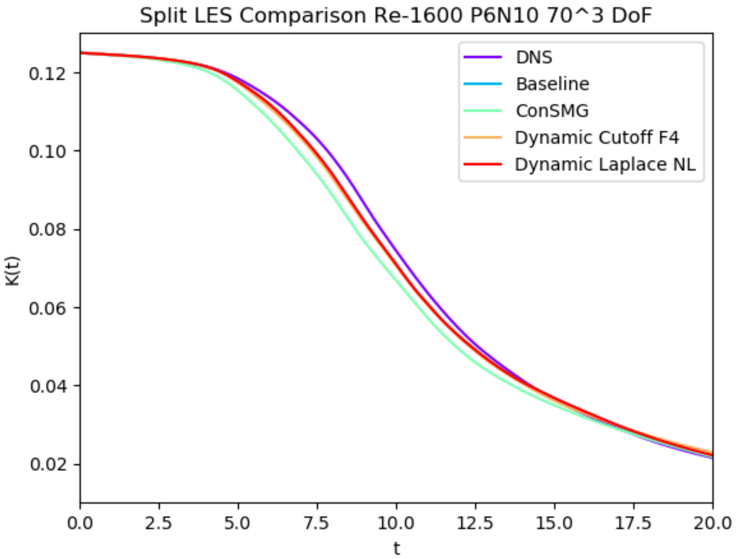

Results: TGV Split-form

- Energy dissipation rate at Re=1,600
  - DNS results are in purple
  - Baseline simulation with no LES model is shown in Blue
  - The simulation with Constant Smagorinsky model is green
  - The simulation with Dynamic Smagorinsky model with the modal cutoff filter set to P4 is in orange
  - The simulation with Dynamic Smagorinsky model with the Laplacian filter is in red

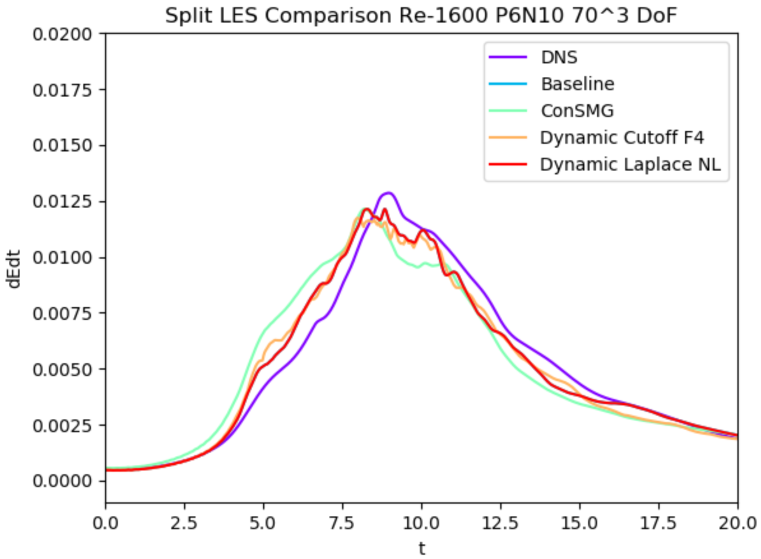

Results: TGV Split-form

- All simulations over predict energy dissipation and predict transition earlier than the DNS
- The Constant Smagorinsky model is the most dissipative until $\tau \approx 7.5$
  - After this time it is the least dissipative

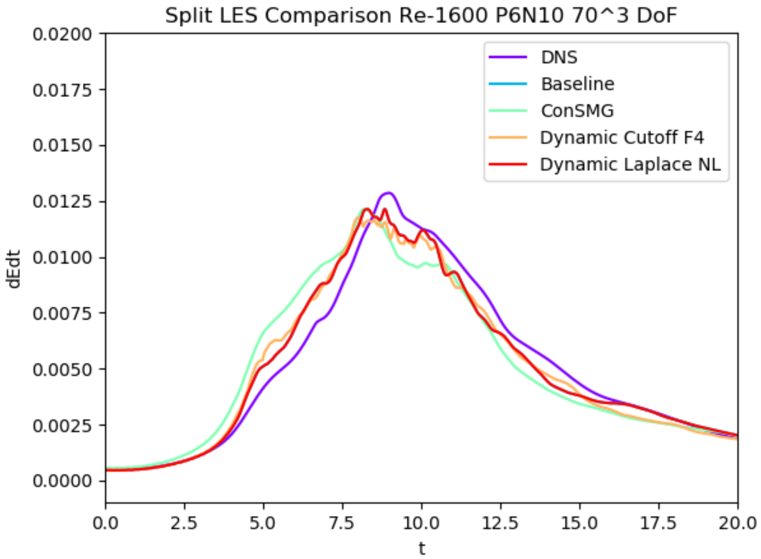

Results: TGV Split-form

- The Dynamic Smagorinsky model with the cutoff filter has close performance with the baseline
  - At $\tau \approx 5$ it is slightly more dissipative, this is responsible for the divergence seen in the figure of TKE shown previously
- The Dynamic Smagorinsky model with the Laplace filter has too small of a contribution and produces negligible differences when compared to the baseline simulation

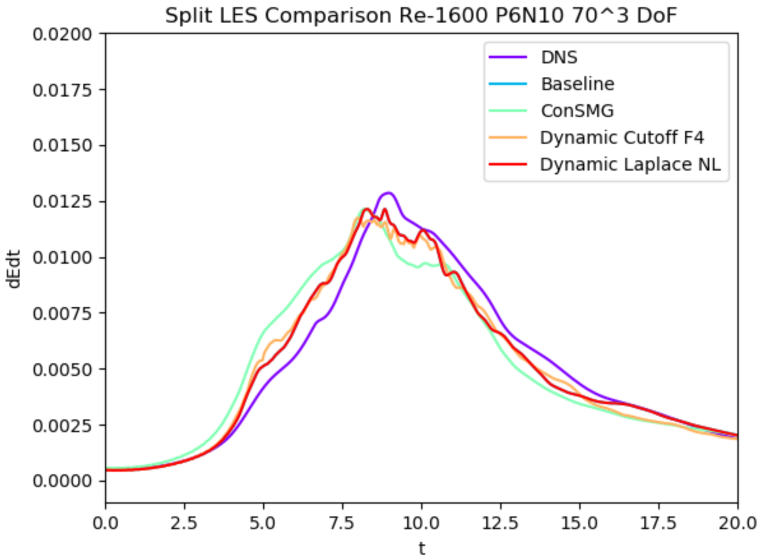

Results: TGV Split-form

- Modeled eddy viscosity is shown
  - This is volume averaged over the whole domain
- The Constant Smagorinsky Model results are shown in purple
- The Dynamic Smagorinsky Model results with the modal cutoff filter is shown in green
- They Dynamic Smagorinsky Model results with the Laplace filter is shown in red

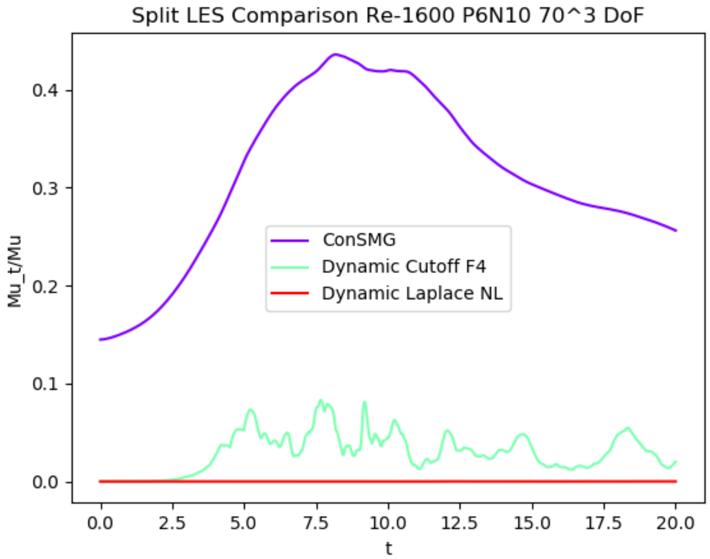

Results: TGV Split-form

- The Constant Smagorinsky model predicts the largest μ_t during the entire simulation
- The Dynamic Smagorinsky model with the cutoff filter predicts a $\mu_t \approx 0$ until $\tau \approx 2.5$
  - This is when the flow is Laminar
- The Dynamic Smagorinsky model with the Laplace filter predicts $\mu_t \approx 0$ for the lifetime of the simulation
  - A closer examination shows similar behavior to the modal cutoff filter
  - The magnitude is too small to have an effect on the flow

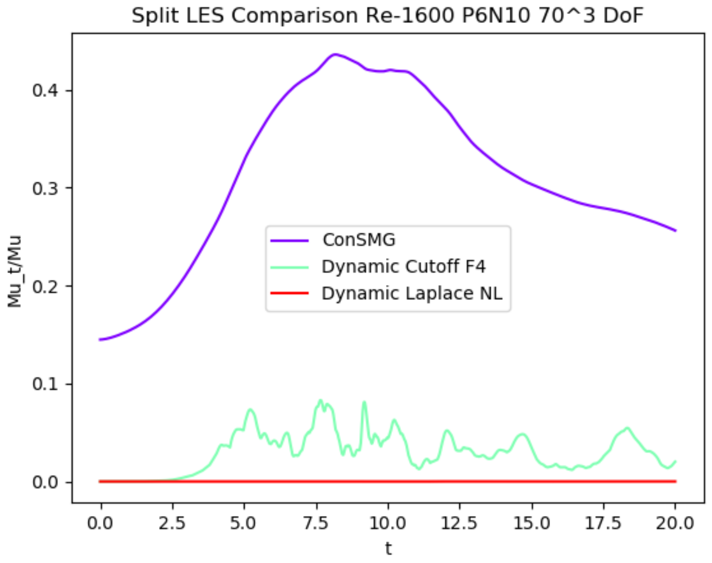

Results: TGV Split-form High Re

- Total Kinetic Energy at Re=20,000
  - DNS results are in purple
  - Baseline simulation with no LES model is shown in Blue
  - The simulation with Constant Smagorinsky model is green
  - The simulation with Dynamic Smagorinsky model with the Laplacian filter is in orange
  - The simulation with Dynamic Smagorinsky model with the modal cutoff filter set to P4 is in red

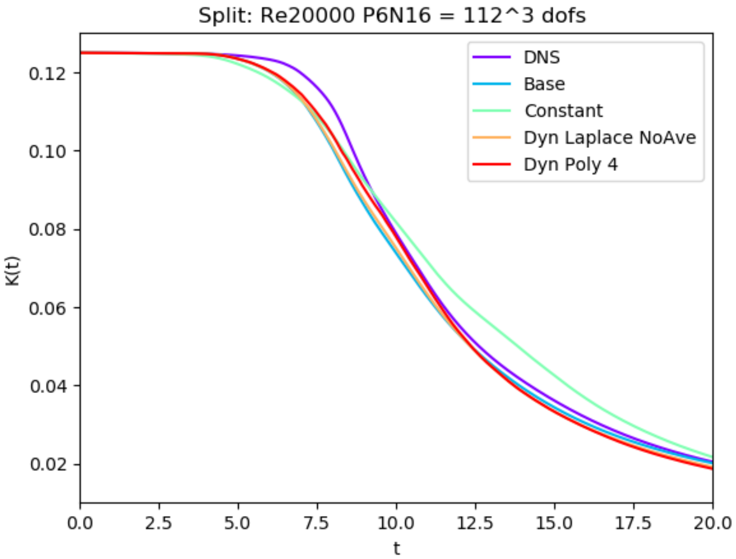

Results: TGV Split-form High Re

- Again, all cases under predict KE and predict transition earlier than the DNS
- The Constant Smagorinsky Model predicts the transition the earliest
  - After transition it over predicts KE

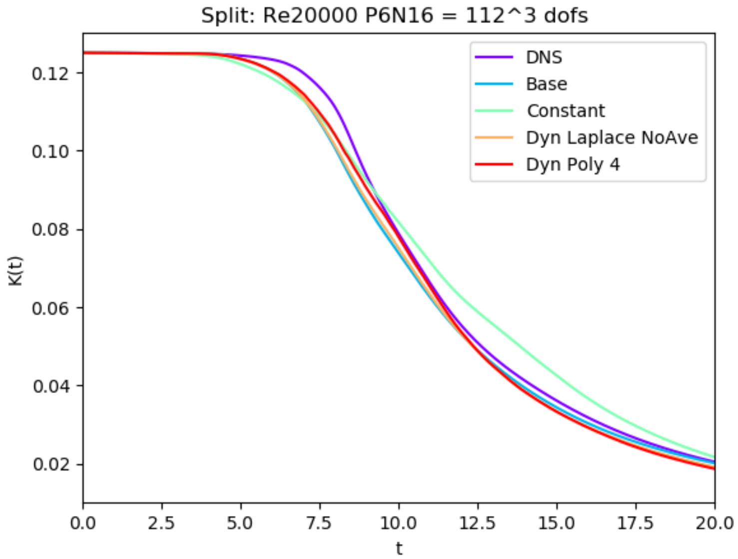

Results: TGV Split-form High Re

- The Dynamic Smagorinsky with the Laplace filter is notably different than the baseline simulation with no LES model
  - Improvement over the lower Reynolds Number case
  - It predicts a higher KE than the baseline
  - Transition occurs at nearly the same time as the baseline
- The Dynamic Smagorinsky with the cutoff filter predicts transition closer to the DNS results than all other cases

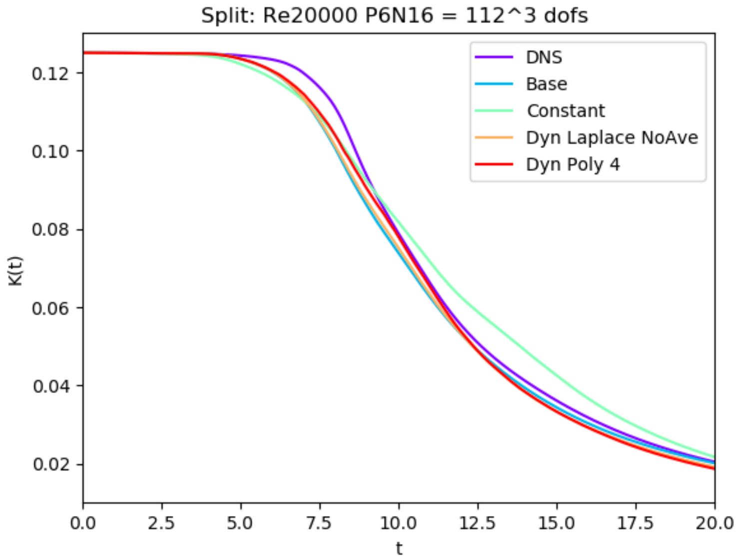

Results: TGV Split-form High Re

- Energy dissipation rate at Re=20,000
  - DNS results are in purple
  - Baseline simulation with no LES model is shown in Blue
  - The simulation with Constant Smagorinsky model is green
  - The simulation with Dynamic Smagorinsky model with the Laplacian filter is in orange
  - The simulation with Dynamic Smagorinsky model with the modal cutoff filter set to P4 is in red

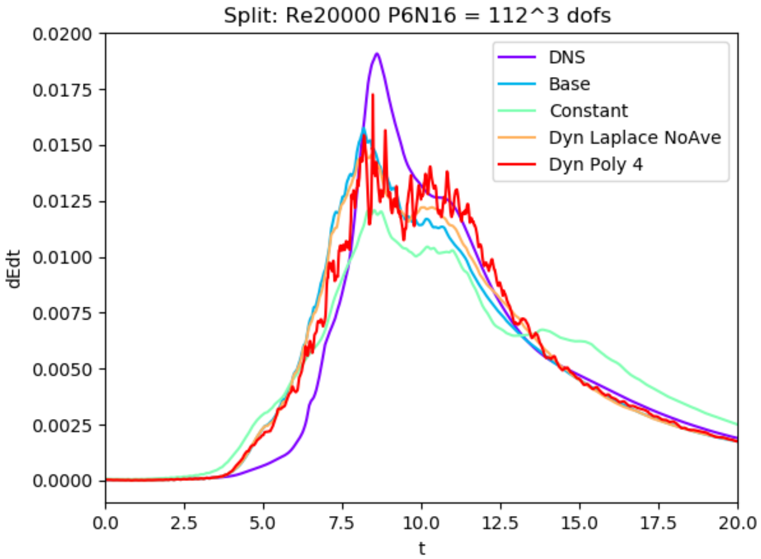

Results: TGV Split-form High Re

- All cases predict a higher dissipation rate before transition
  - $\tau \approx 7.5$
- After this point they under predict the energy dissipation rate until $\tau \approx 13.0$
- The DNS indicates there is a secondary peak at $\tau \approx 12.0$
  - This is not seen in the lower Re case
  - All LES cases capture this

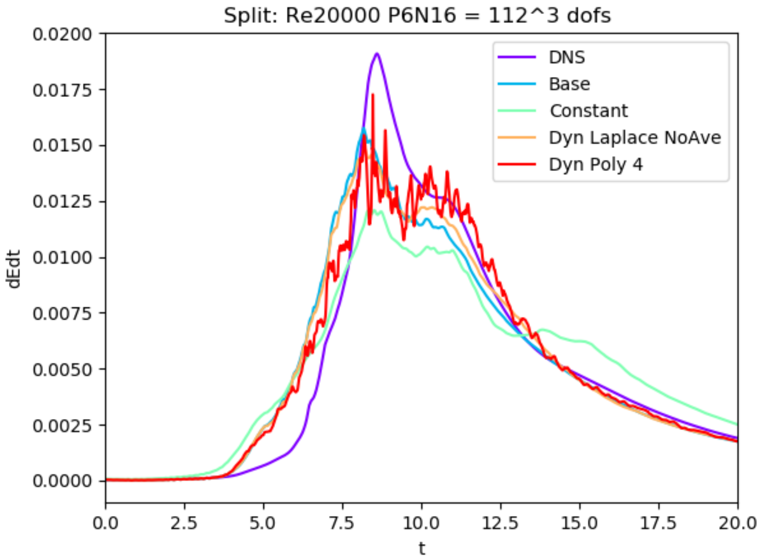

Results: TGV Split-form High Re

- The Constant Smagorinsky Model predicts the onset of transition the earliest
    - After $\tau \approx 6.0$ it predicts the lowest dissipation rate of the LES cases
- The Dynamic Smagorinsky Model case with the cutoff behaves similarly to the baseline no model case until $\tau \approx 6.0$
    - This case also has a significant amount of fluctuations after $\tau \approx 6.0$

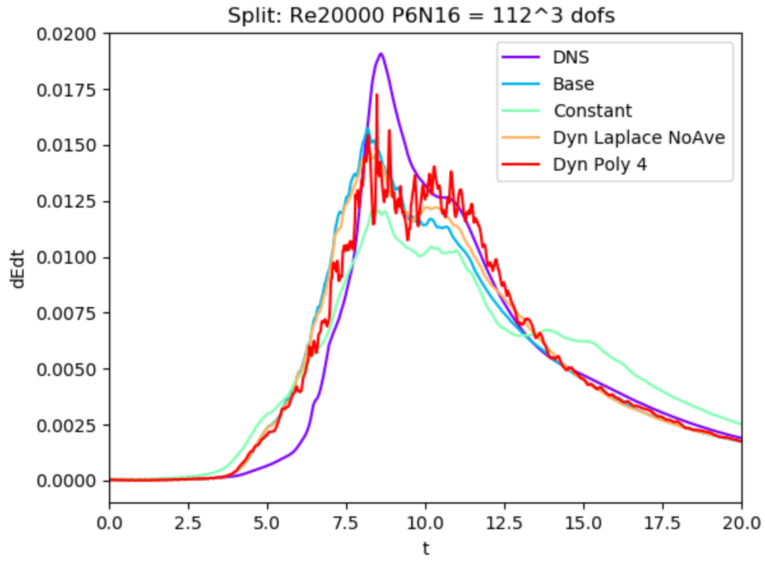

Results: TGV Split-form High Re

- The Dynamic Smagorinsky Model case with the Laplace filter behaves similarly to the baseline no model case until $\tau \approx 9.0$
  - Unlike the Low Re case this filter has a significant contribution
  - In many areas this case performs closer to the DNS results than the other LES cases

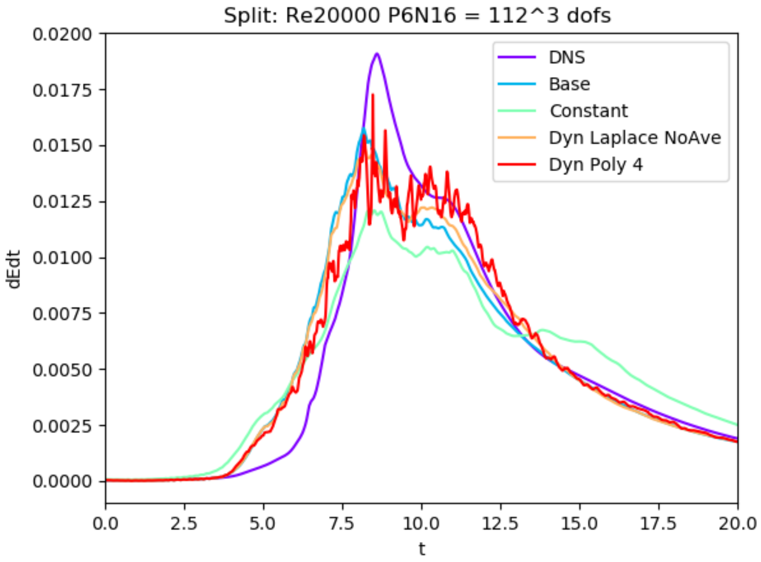

Results: TGV Split-form High Re

- Modeled eddy viscosity is shown
  - This is volume averaged over the whole domain
- The Constant Smagorinsky Model results are shown in purple
- The Dynamic Smagorinsky Model results with the modal cutoff filter is shown in green
- They Dynamic Smagorinsky Model results with the Laplace filter is shown in red

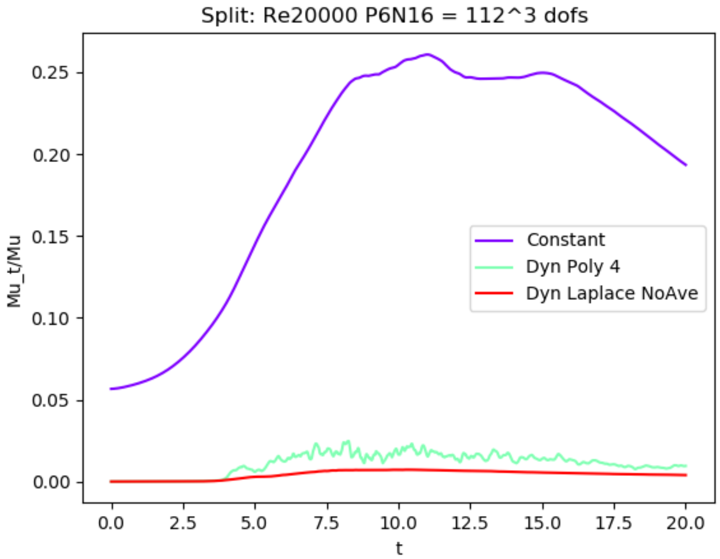

Results: TGV Split-form High Re

- As seen in the low Re case the Constant Smagorinsky model predicts the largest μ_t during the entire simulation
- The Dynamic Smagorinsky model case with the modal cutoff filter predicts a near zero μ_t until about $\tau \approx 4.0$
  - This is desirable as the flow is laminar early in the simulation
- The Dynamic Smagorinsky model case with the Laplace filter again has the lowest volume averaged μ_t
  - Unlike the low Re Case μ_t has a notable contribution on the flow

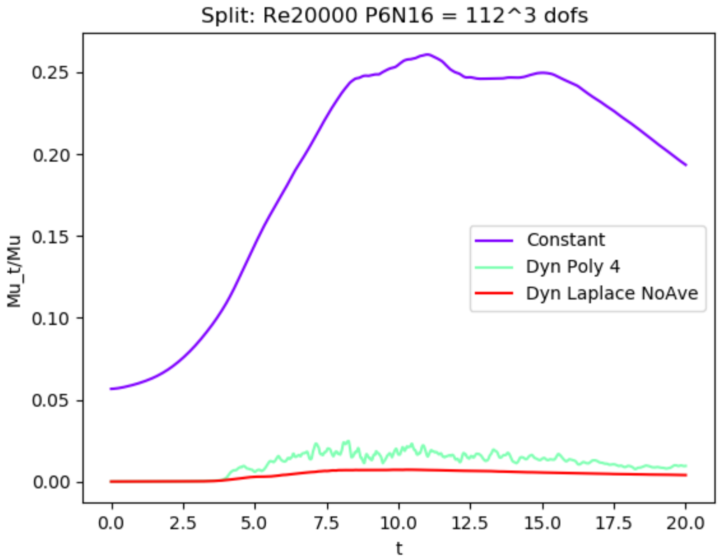

Conclusions

- The standard DG discretization is unstable for the inviscid TGV
  - It is unstable in every case
- The split-form discretization can preserve KE
  - This is seen in the inviscid TGV
    - No dissipation was added with a numerical flux scheme
    - Some cases were stable for the whole simulation life with negligible loss in KE
- The standard DG discretization is unstable when the split-form discretization is stable
  - When the stand DG discretization is stable it is less dissaptive than the split-form discretization

Conclusions

- At Re=1600 all LES models under predict KE when compared to the DNS results
  - The case with no LES model was the least dissipative
- At Re=20000 all LES models under predict KE when compared to the DNS results
  - The Dynamic Smagorinsky model cases had less dissipation than the no model LES case
    - This arises from the extra dissipation from the model is applied in key flow areas

Conclusions

- The Constant Smagorinsky Model was the most dissipative when compared to the Dynamic Smagorinsky model and no model cases
  - This model has poor performance for laminar flows
- The Dynamic Smagorinsky model cases performed better than the Constant Smagorinsky Model case
  - This model has better performance in laminar flows
  - Accurately capturing the early laminar flow and transition leads to better accuracy

Future Work

- The split-form discretization chosen was kinetic energy preserving
  - Other discretizations exist with different variable formulations or preserved properties
- Other LES models should be explored
  - Dynamic Heinz
  - Wall-Adapting Local Eddy-Viscosity (WALE) model
- Other turbulent flow problems should be analyzed
  - Turbulent channel flow

Acknowledgements

- Advisor: Dr. Dimitri Mavriplis
- Committee:Dr. Michael K. Stoellinger and Dr. Stefan Heinz
- Dr. Andrew Kirby
- Labmates: Soudeh Kamali, Emmettt Padway, Donya Ramezanian
- Rajib Roy, Arash Hassanzadeh, and Dr. Jonathan Naughton

Acknowledgements

- Office of Naval Research
  - ONR Grant N00014-14-1-0045
- U.S. Department of Energy, Office of Science, Basic Energy Sciences
  - Award DE-SC0012671
- Compute Time
  - NCAR-Wyoming Supercomputer Center (NWSC)
    - *doi:10.5065/D6RX99HX*
  - University of Wyoming Advanced Research and Computing Center (ARCC)

Questions

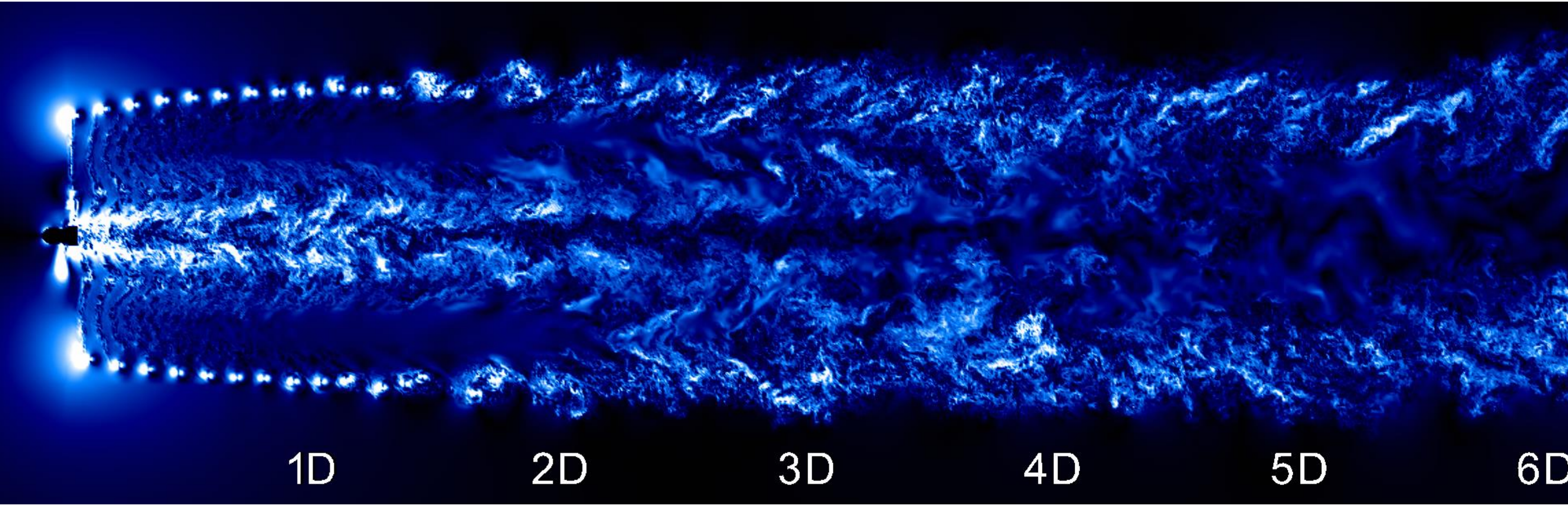

References

1. Wang, Z. J., Fidkowski, K., Abgrall, R., Bassi, F., Caraeni, D., Cary, A., Deconinck, H., Hartmann, R., Hillewaert, K., Huynh, H., Kroll, N., May, G., Persson, P.-O., van Leer, B., and Visbal, M., \High-order CFD methods: current status and erspective," International Journal for Numerical Methods in Fluids, Vol. 72, No. 8, 2013, pp. 811845.